ECS Transactions, 18 (1) 213-218 (2009)
10.1149/1.3096452 ©The Electrochemical Society

Si-O bond-breakage energetics under consideration of the whole crystal

S.E. Tyaginov[a], V. Sverdlov[b], W. Gös[a], Ph. Schwaha[b],
R. Heinzl[b], F. Stimpfl[b], T. Grasser[a]

[(a)]Christian Doppler Laboratory for TCAD at the [(b)]Institute for Microelectronics,
TU Wien, Gußhausstraße 25-29, A-1040 Vienna, Austria

We extend the McPherson model for Si-O bond-breakage energetics, which considers only a single SiO_4 tetrahedron, in a way to capture the effect of the whole crystal. No ledge in the direction assumed in the McPherson model was revealed. Instead, potential profiles feature a saddle point in a different direction. The activation energy for bond-breakage is found to be rather high (~ 6 eV). This suggests that the interaction with the electric field alone is not sufficient for bond rupture. The breakage rate calculated for a bond weakened by hole capture is comparable to that of the McPherson model. We conclude that only the common action of an electric field and other factors (structural disorder and/or energy delivered by particles, e.g. hot carriers) can result in bond-breakage.

1. Introduction

Two main concepts of the breakdown of SiO_2 film exist in the literature: the first one relates the dielectric degradation with energy delivered by particles and the second one treats the interaction with the electric field as the triggering mechanism for oxide damage. One may distinguish two main approaches supporting the first concept – namely the Anode Hole Injection model (1,2) and the Anode Hydrogen Release model (3,4) – while the Electro-Chemical model (5,6) treats the Si-O bond-breakage in terms of a chemical reaction where the activation energy is lowered by the field. At the same time, the rupture of Si-O bonds has been suggested to be an essential component of the Hot Carrier induced degradation (7,8) and of the Time Dependent Dielectric Breakdown (5,6) and thus the model of Si-O bond breakage is the one of the crucial challenges in the area of SiO_2 film reliability. The McPherson model (5,6) treats the rupture of Si-O bonds as a transition of the Si ion from the 4-fold position to the 3-fold coordination. This model, however, considers only a single SiO_4 tetrahedron. It is obvious that the contribution of the whole surrounding network substantially changes the situation. For instance, neighboring Si ions are situated in a distance of ~ 3.2 Å from the center of the tetrahedron and carry the charge twice as large as that of the O ions. Thus the contribution to the energy of each Si ion is comparable to that provided by the O ions. In this work the McPherson model will be extended in a way to capture the effect of the whole lattice.

2. Generalization of Mie-Grüneisen Potential

Following McPherson, we employ the Mie-Grüneisen potential (MGP) (5,6) to describe pair-wise interatomic interactions in SiO_2. However, we take into account not only Si-O, but also Si-Si and O-O interactions and use the MGP in a generalized form:

$$\Phi_{ij}(r_{ij}) = Q_i^{(9)} Q_i^{(9)} r_{ij}^{-9} + Q_i^{(2)} Q_i^{(2)} r_{ij}^{-2} + Q_i^{(1)} Q_i^{(1)} r_{ij}^{-1}, \qquad [1]$$

where the indices *i,j* indicate the type of the atom, r_{ij} is the interatomic distance and $Q_i^{(m)}$ are "effective charges" of ions corresponding to the term of the *m*-th power. We have 6 constants to be determined (2 types of ions with each characterized by 3 parameters).

The number of independent constants is further reduced by the requirement of finiteness of the electrostatic energy (for each *m*):

$$U^{(m)} = \frac{1}{2} \sum_{n_1,n_2,n_3} \sum_i \sum_j \frac{Q_i^{(m)} Q_j^{(m)}}{|\vec{r}_i - \vec{r}_j + \vec{n}|^m}, \qquad [2]$$

where *i,j* enumerate ions in a primitive cell, $\boldsymbol{r}_i$, $\boldsymbol{r}_j$ are the positions of the atoms and $\boldsymbol{n} = n_2\boldsymbol{t}_2 + n_2\boldsymbol{t}_2 + n_3\boldsymbol{t}_3$ with $\{\boldsymbol{t}_1,\boldsymbol{t}_2,\boldsymbol{t}_3\}$being basis translation vectors. These series converge only when the unit cell is neutral, i.e. presuming that it contains 3 Si and 6 O atoms, one writes $Q_{Si}^{(m)} / Q_O^{(m)} = -2$ for each *m* and as a consequence only 3 independent constants remain.

The McPherson model uses 3 constants, which are found by the condition that the potential energy has a minimum at the Si equilibrium position (EP) (zero force on the Si ion and the energetic position of the minimum is equal to the bond strength) and the bond polarity must represent the conventional value for the Si-O bond. The constant set used in the original model is not applicable in the extended version because it results in a wrong value of the cohesion energy. Also the potential acting on the O ion reveals an energy maximum instead of a minimum at the EP. To determine $Q_i^{(m)}$ a calibration scheme reproducing some material characteristics (cohesion energy and elastic constants) has to be employed. Another suitable way is to calibrate the MGP results to the data obtained by the Density Functional Theory (DFT) combined with the Molecular Dynamics (MD). However, a more straightforward way is to employ TTAM and BKS interatomic potentials which have been designed just to reproduce results of DFT/MD (9-12).

3. TTAM and BKS potentials

The general expression for TTAM and BKS potentials contains 3 terms: the Coulombic, the covalent, and the short-range repulsive term precluding the collapse of atoms:

$$\Phi_{ij}(r_{ij}) = \frac{kQ_iQ_j}{r_{ij}} + \alpha_{ij} e^{-\beta_{ij} r_{ij}} - \gamma_{ij} r_{ij}^{-6}. \qquad [3]$$

The constant *k* converts $e^2Å^{-1}$ to eV. As in [1], indices *i,j* enumerate the types of the atoms. We employ only the versions of potentials based on commonly-accepted values of Q_{Si}/Q_O = +2.4/-1.2 (in electron charge) as effective charges in the Coulombic term. Diverse forms of TTAM/BKS differ in values of constants α_{ij}, β_{ij}, γ_{ij} listed in the Table I (9-12).

The potential acting on the Si ion from the rest of the crystal vs. its displacement from the EP perpendicular to the O_3 plane is shown in Fig. 1a and toward the middle of the O-O segment is depicted in Fig 1b. In the direction declared in the McPherson model no saddle point is observed. Instead, the secondary minimum/ledge is revealed for the

second direction for all types of potentials. The activation energy needed for the Si atom to transfer from the 4-fold coordination to the 3-fold position is rather high, i.e. ~ 6 eV vs. ~ 2.3 eV found in (5,6). This circumstance is related to the effect of the surrounding network, primarily, to the presence of 4 neighboring Si ions providing a strong positive contribution to the potential. Although energy positions of the primary minimum and the ledge are different for various potentials, the activation energies for bond-breakage are approximately the same. We use the classical version of the TTAM potential further on.

TABLE I. Values of constants used in various versions of TTAM/BKS potentials (9-12)

Version of the potential	α_{ij}	β_{ij}	γ_{ij}
Si-Si TTAM	$8.7235 \cdot 10^{8}$	15.2207	23.30
Si-Si BKS	0	0	0
Si-Si Z1-TTAM	0	0	0
Si-Si FB-TTAM	$7.950 \cdot 10^{4}$	4.975	446.780
Si-O TTAM	10721.5	4.7959	70.7343
Si-O BKS	18003.8	4.8738	133.538
Si-O Z1-TTAM	7149.0	4.7864	27.661
Si-O FB-TTAM	10450.0	4.8077	63.047
O-O TTAM	1756.90	2.8464	214.736
O-O BKS	1388.773	2.760	175.00
O-O FB-TTAM	1428.0	2.7933	41.374
O-O Z1-TTAM	1359.0	2.8086	215.829

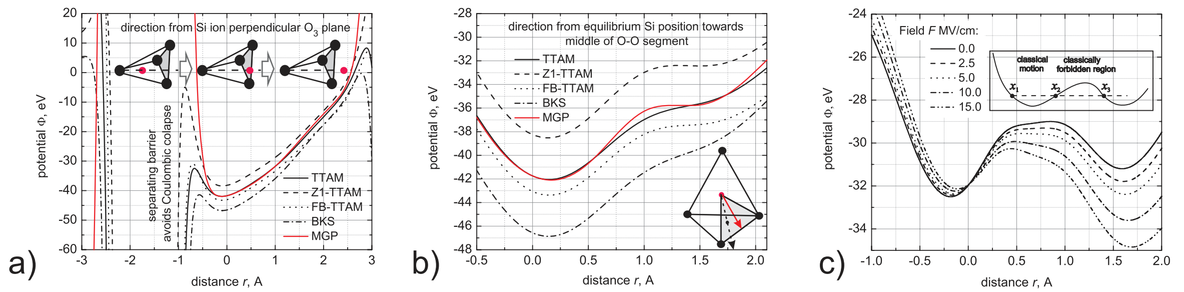

Figure 1. The potential acting on the Si ion vs. its displacement from the EP: (a) perpendicular to the O_3 plane (see inset); (b) toward the middle of the O-O segment (inset: red arrow, black arrow – McPherson direction); (c) transformation of the potential with the electric field (bond is weakened by HC).

4. Calibration of Mie-Grüneisen Potential

For both types of ions the potential acting on them should reveal a minimum at their EP. We employ the energy positions of the corresponding minima for Si and O ions as well as the cohesion energy of α-SiO_2 (the values published in the literature span the range from 18 to 19.1 eV/formula unit (13-15); 19.1 eV/formula unit, Ref. (15) is used in this work) to find 3 constants in the MGP. It is more convenient to find the products $Q_{Si}^{(m)}Q_{O}^{(m)}$ ($Q_{O}^{(m)}Q_{O}^{(m)}$ = -1/2 $Q_{Si}^{(m)}Q_{O}^{(m)}$, $Q_{Si}^{(m)}Q_{Si}^{(m)}$ = -2 $Q_{Si}^{(m)}Q_{O}^{(m)}$) rather then the $Q_{Si}^{(m)}$, $Q_{O}^{(m)}$ separately. Table II compares the values found in this work with those from the McPherson model. Note that we have rewritten the dimensionless constants used in (5) in terms of $Q_{Si}^{(m)}Q_{O}^{(m)}$.

The potential for the Si ion calculated with properly-parameterized MGP is shown in Fig. 1a-b for the direction assumed in the McPherson model and that revealed in the present extended version, respectively. One can see that also with MGP employed no ledges are revealed in the first case while in the direction from the Si EP towards the middle of the O-O segment the secondary minimum is observed at the same positions as with

TTAM/BKS. We intentionally did not include the secondary minimum into the calibration procedure to avoid its artificial appearance predefined by the calibration.

TABLE II. Comparison of the MGP constants employed in the McPherson model and those used in the present model.

Power of term *m*	McPherson Model	Present model
9	117.964 eV·Å^9	99.480 eV·Å^9
2	-7.392 eV·Å^2	-3.148 eV·Å^2
1	-6.523 eV·Å	-41.308 eV·Å

5. Effect of hole capture and electric field

As it was reported in the original McPherson model, the effective dipole moment lies in the range of 7…13 *e*Å and thus the dipole – electric field interaction could change the potential energy by ~ eV. Keeping in mind the huge activation energy of ~ 6 eV for bond-breakage obtained in our model, we conclude that the electric field $\boldsymbol{F}$ only is not sufficient for the rupture of Si-O bonds and the contribution of other factors is essential for effective bond-breakage. One of the possible candidates may be a bond weakening by hole capture (HC) and, thus, we consider the transformation of the Si binding potential with the electric field for a bond distorted by HC.

We assume a captured hole is situated in the middle of the Si-O bond and its contribution into the potential ($\boldsymbol{r}_{Si}/\boldsymbol{r}_O$ are the position of the Si/O ion, $\varepsilon_0\varepsilon_I = 3.9$ is the permittivitiy) is:

$$\Phi_{hole} = \frac{+|e|\cdot Q_{Si}}{4\pi\varepsilon_o\varepsilon_I\left|\vec{r}_{Si} - 1/2(\vec{r}_{Si} - \vec{r}_O)\right|} = \frac{+|e|\cdot Q_{Si}}{8\pi\varepsilon_I\varepsilon_0\left|\vec{r}_{Si} - \vec{r}_O\right|}, \quad [4]$$

With Si being in the EP the dipole moment $\boldsymbol{p} = \boldsymbol{0}$ but it develops as Si is shifted. Since the Si/O ions have a charge of $+4|e|f_i^*/-2|e|f_i^*$ (f_i^* is the bond polarity; *i* enumerates 4 O atoms bonded to the Si) the contribution to the potential due to the interaction with the field is:

$$\Phi_{dip}(\vec{r}) = -\vec{p}\cdot\vec{F} = -2|e|\left[\sum_{i=1}^{4} f_i^*(\vec{r} - \vec{r}_i)\right]\left(\frac{2+\varepsilon_I}{3}\right)\vec{F}. \quad [5]$$

Similarly to the McPherson model, we assume that the bond polarity changes if the Si ion is displaced from its EP as $f_i^* = \frac{f_o^*}{\left(1 - f_o^*\right)\left(r_0/r\right) + f_o^*}$, where f_0^* is the bond polarity in equilibrium, $r_0 = 1.7$ Å is the bond length and *r* is the ion displacement.

The transformation of the potential profile $V(x)$ of the Si ion calculated for a bond weakened by HC with the applied field *F* is depicted in Fig. 1c. The degeneracy of the two minima occurs at F_{cr} ~ 5 MV/cm. Comparing this value with one reported in the McPherson model (15 MV/cm) one concludes that our critical field is more realistic, because 15 MV/cm is even higher than the dielectric strength of silica ~ 10 MV/cm (16).

6. Quantization effects and bond-breakage probability

Following McPherson, we treat the rupture of the Si-O bond as a transition of the Si ion from the 4-fold coordinated position to the 3-fold coordination outside the SiO_4 tetrahedron. We assume that two processes contribute to bond-breakage: thermal activation of the Si ion over the barrier separating the primary and the secondary minima

and its tunneling through the barrier as in the McPherson model. The second mechanism will be treated quasi classically, i.e. within the WKB approximation.

In the quantum well corresponding to the primary minimum there is a system of energy levels; each level is characterized by its energy E_n, occupancy f_n, allez-retour time $\tau_{a\text{-}r,n}$, and the probability T_n to tunnel through the barrier are found from:

$$\int_{x_1}^{x_2} \sqrt{2m_{Si}\left(E_n - V(x)\right)dx} = (n+1/2)\pi\hbar\,, \tag{6a}$$

$$f_n = \exp(-E_n / k_B T) / \sum_n \left[\exp(-E_n / k_B T)\right] \tag{6b}$$

$$\tau_{a-r,n} = 2\sqrt{\frac{m_{Si}}{2}} \int_{x_1}^{x_2} \frac{dx}{\sqrt{E_n - V(x)}} \tag{6c}$$

$$T_n = \exp\left(-\frac{2}{\hbar} \int_{x_2}^{x_3} \sqrt{2m_{Si}\left[V(x) - E_n\right]} dx \right), \tag{6d}$$

m_{Si} is the mass of the Si ion, $\{x_1,x_2\}$ and $\{x_2,x_3\}$ are points limiting the classically allowed and prohibited regions of Si motion (Fig. 1c, inset). The tunneling rate from each level is expressed as $P_n = f_n T_n / \tau_{a\text{-}r,n}$. Note that the contribution to the bond-breakage process by thermionic emission is negligibly small with respect to tunneling, because the relatively high and narrow barrier is rather "suited" for tunneling than for thermal activation.

The level position as a function of its quantum number is presented in Fig. 2a; the number of levels decreases with F when the quantum well becomes shallower. Since tunneling occurs only from levels situated above the bottom of the 2nd minimum the offset of tunneling is observed in Fig 2b which shows P_n as a function of F. The trade-off between rapidly increasing with E_n tunneling transparency T_n and decreasing occupancy f_n reveals that the main contribution to the total rate P_n is due to 2-3 first levels. Fig 2c compares the total bond-breakage rate calculated in the present model for a bond weakened by HC and that borrowed from (6) (multiplied by an attempt rate $v \sim 10^{13}$ s).

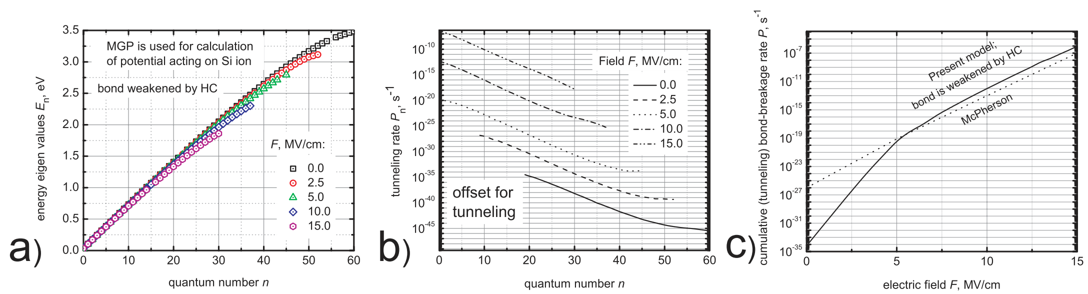

Figure 3. Bond-breakage energetics: (a) the system of energy levels; (b) tunnel rate vs. the level number for various F; (c) bond-breakage rates obtained with the McPherson model for a "virgin" bond vs. that obtained in our model for a bond weakened by HC.

Fig. 2c demonstrates similar rates obtained for 2 principally different cases: with and without bond weakening by HC. The McPherson model considers only a single tetrahedron. This suggests that under the consideration of the whole crystal the

interaction with an electric field could not provide a considerable bond-breakage rate and only its combined action with other factors such as structural disorder (HC, bond angle variations, bond stain) and/or energy delivered by particles (hot carriers, mobile hydrogen) results in bond rupture.

7. Conclusion

An extended version of the McPherson model which captures the effect of the whole crystal on Si-O bond-breakage energetics has been developed. Similar results were obtained with several types of pair-wise potentials. It was revealed that the surrounding network strongly stabilizes the SiO_4 tetragonal bonding configuration. No saddle point in the McPherson direction was observed. Instead a saddle point appears in the direction connecting the center of the SiO_4 tetrahedron and the middle of the O-O segment. The degeneracy of the primary and the secondary minima occurs at lower fields than in the McPherson model, i.e. at ~ 5 MV/cm. The barrier separating the two minima is too high for the thermal activation. Therefore, the interaction of the dipole moment with an electric field is not able to provide a significant rate for bond-breakage. Thus, the common action of a field and other factors is required for bond rupture. Among these factors are bond weakening by hole capture, bond angle deviations, bond strain, etc as well as energy deposited by particles, primary by hot carriers and mobile hydrogen. It is shown that the bond-breakage rate calculated within the McPherson model for a "virgin bond" and within the present model for a bond weakened by hole capture can be similar.

References

1. M. Alam, J. Bude, A, Ghetti, *38th Intern. Reliab. Phys. Symp.*, p. 21 (2000).
2. J. Bude, B. Weir, P. Silverman, *IEDM Tech. Dig.*, p. 179 (1998).
3. D.J. DiMaria, J.H. Stathis, *J. Appl. Phys.*, **89**, 9, p. 5015 (2001).
4. A. Ghetti, M. Alam, J. Bude, D. Monroe, E. Sangiorgi, H. Vaidya, *IEEE Trans. Electron Dev.*, **47**, **7**, p. 1341 (2000).
5. J.W. McPherson, *J. Appl. Phys*., **99**, 8, pap. No. 083501, 13 pages (2006).
6. J.W. McPherson, *45th Inter. Reliab. Phys. Symp.*, p. 209 (2007).
7. S. Mahapatra, D. Saha, D. Varghese, P.B. Kumar, *IEEE Trans. Electron Dev*., **53**, 7, p. 1583 (2006).
8. D. Saha, D. Varghese, S. Mahapatra, *IEEE Electron Dev. Lett*., **27**, 7, p. 585 (2006).
9. S. Tsuneyuki, M. Tsukada, H. Aoki, Y. Matsui, *PRL.*, **61**, 7, p. 869 (1998).
10. B.W.H. van Beest, G.J. Kramer, R.A. van Santen, *PRL*. **64**, 16, p. 1955 (1998).
11. A.R. Al-Derzi, M.G. Gory, K. Runge, S.B. Trickey, *J. Phys. Chem*. A, **108**, 52, p. 11679 (2004).
12. W. Zhu, K. Runge, S.B. Trickey, *J. Comp.-Aid. Mater. Design*, **13**, 1-3, p. 75 (2006).
13. A. Tandia, G. Sarrabayrouse, A. Martinez, *Thin Solid Films*, **296**, 1-2, p. 122 (1997).
14. F. Jollet, C. Noguera, *Phys. Stat. Sol. (b)*, **179**, 2, p. 473 (1993).
15. Sh. Munetoh, T. Motooka, K. Moriguchi, A. Shintani, *Comput. Mat. Sci.*, **39**, 2, p. 334 (2007).
16. S.M. Sze, K.K. Ng, *Physics of Semiconductor Devices*, 3rd edition, Wiley and Sons, New-York, 2006.